J. Fluid Mech. (1997), *vol.* 339, *pp.* 275–285

On the origin of the 'surface current' in turbulent free-surface flows

By DAVID T. WALKER

Earth Sciences Group, Environmental Research Institute of Michigan, PO Box 134001, Ann Arbor, MI 48113-4001, USA *and* Department of Naval Architecture and Marine Engineering, University of Michigan, Ann Arbor, MI 48109-2145, USA

(Received 1 August 1996 and in revised form 9 January 1997)

In this study, the interaction with a free surface of an initially axisymmetric jet issuing beneath and parallel to the surface was examined. The purpose was to determine the origin of the 'surface current' – the large outward velocity which exists in a thin layer adjacent to the surface. Using the equations of mean motion, it is shown that near the surface, outward acceleration results from the balance between a positive contribution from the lateral Reynolds-stress gradients and a negative contribution from the lateral pressure gradient. The local pressure field near the free surface is shown to be largely determined by the local Reynolds-stress field. Combining these results shows that the lateral acceleration which results in the surface current is related to the Reynolds-stress anisotropy near the surface. The results indicate that there should be roughly a three-fold increase in the lateral growth rate of the jet near the free surface and a similar increase in the outward velocity, when compared to a deep jet. Comparison to available experimental data showed that the maximum outward velocity was consistent with the theory, and that the lateral scale of the surface-current layer was roughly double that of the deep jet, slightly smaller than expected. The near-surface stress anisotropy was shown to be related to the interaction of vorticity with the free surface. This indicates that the results of this study are consistent with earlier explanations of the surface current in terms of vortex/free-surface interaction.

1. Introduction

When a turbulent shear flow such as a jet or a wake evolves near a free surface, a vertically thin region of large transverse (outward) velocity develops adjacent to the surface. This feature, dubbed the 'surface current' by Anthony & Willmarth (1992), has been observed in model-ship wakes (Walker & Johnston 1991), free-surface jets (Anthony & Willmarth 1992; Walker, Chen & Willmarth 1995), and wakes of surface-piercing flat plates (Logory, Hirsa & Anthony 1996). Similar behaviour has also been observed in a temporally evolving round jet (Mangiavacchi, Gundlapalli & Akhavan 1994). Thus, the 'surface current' appears to be a ubiquitous feature of turbulent free-surface flows.

The origin of this outward flow has never been fully established. Visualization studies have related it to the interaction of tangential vorticity with the free surface (Walker *et al.* 1995; Mangiavacchi *et al.* 1994) as have studies based on near-surface vorticity measurements (Logory *et al.* 1996). Walker *et al.* (1995) proposed that this vortex/free-surface interaction could be related formally to the anisotropy of the turbulence near the free surface. Both Davis & Winarto (1980) and Launder & Rodi (1983) observed similar spreading near the wall in initially axisymmetric wall jets. Launder & Rodi

(1983) conjectured that this phenomenon has its origin in the production of streamwise vorticity by Reynolds-stress gradients. The occurrence of similar results in both wall jets and free-surface jets led Anthony & Willmarth (1992) to conclude that the surface current must be caused by the common kinematic boundary condition on the surface-normal velocity (i.e. the surface-normal velocity vanishes at the boundary) not the differing conditions on the tangential velocities.

For this study, the case of an initially axisymmetric jet issuing below and parallel to a free surface is chosen, althought the results are expected to be somewhat general. In §2, below, it is shown, through an order-of magnitude analysis of the Reynolds-averaged equations of motion, that the origin of the surface current can be traced to the anisotropy of the turbulence caused by the kinematic free-surface boundary condition. In addition, estimates of the magnitude of the outward velocity and the lateral growth rate of the near-surface layer are developed. In §3, these results are shown to compare favourably with available low-Froude-number jet data. The results are then related to vortex/free-surface interactions in §4. The conclusions are summarized in §5.

2. The free-surface jet

For a turbulent jet issuing beneath a free surface, the jet initially evolves in a manner similar to a jet in an unbounded medium – a 'deep' jet. Eventually the jet begins to interact with the free surface. Once interaction with the free surface begins, it will be assumed that except for a thin layer near the surface, the jet behaves as a deep jet. (That this is a reasonable assumption is demonstrated below in §3.) In what follows, the form of the Reynolds-averaged Navier–Stokes (RANS) equations governing the evolution of a deep jet will first be developed, followed by those governing the behaviour of the thin region near the free surface. The results will then be combined to determine the origin of the surface current for this flow.

The RANS equations will be used in the following form, which applies for stationary flow:

$$\overline{U_j}\frac{\partial \overline{U_i}}{\partial x_j} = -\frac{\partial \overline{P}}{\partial x_i} + \nu\frac{\partial^2 \overline{U_i}}{\partial {x_j}^2} - \frac{\partial \overline{u_j u_i}}{\partial x_j}, \tag{2.1}$$

where the overbar indicates a mean quantity, uppercase letters represent instantaneous values, and lowercase letters represent fluctuations relative to the mean. Here, $\overline{P}$ is the mean pressure divided by the density, excluding hydrostatic effects – as a result, there is no explicit body force term in the RANS equations. It will be assumed that the Reynolds number is sufficiently high that viscous effects are negligible, therefore the viscous terms will hereafter be dropped.

For the deep jet, it is assumed that the local characteristic streamwise (x-direction) velocity scale for a jet is $U_\circ$ and that the length scale for variations in the streamwise direction is x, the distance from the jet origin. The length scale for variations in the radial direction for this axisymmetric flow ℓ, defined as the jet half-width at half the maximum velocity, is taken to be smaller than than $x/10$ (see e.g. Wygnanski & Fiedler 1969 for experimental verification). The coordinate system and radial length scale for the deep jet are shown in figure 1(a). From the Reynolds-averaged continuity equation, one can deduce that the scale for the mean radial velocity is of order $U_\circ \ell/x$. The turbulent velocity fluctuations will have a scale of $u_\circ$ which, based on experiment (Wygnanski & Fiedler 1969), is known to be of a magnitude such that $u_\circ^2 \sim U_\circ^2/10$.

These scales can be used to determine the dominant terms in the equations of motion. The analysis for the deep jet is well established (see e.g. Tennekes & Lumley

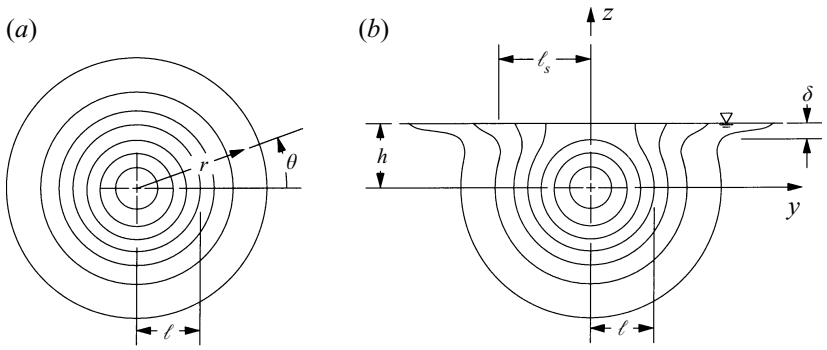

FIGURE 1. Schematic of streamwise velocity contours in a plane normal to the jet axis illustrating length-scale definitions. (*a*) Streamwise velocity contours for a 'deep' jet showing the (r,θ) coordinate system and the characteristic length scale ℓ. (*b*) Streamwise velocity contours for a free-surface jet (after Anthony & Willmarth 1992) showing the (x,y) coordinate system and the characteristic horizontal length scale ℓ_s and vertical length scale δ for the surface-current layer.

1972) and so only the key results will be summarized. The Reynolds-averaged axial (x) momentum equation for stationary flow is

$$\overline{U}_x\frac{\partial\overline{U}_x}{\partial x}+\overline{U}_r\frac{\partial\overline{U}_x}{\partial r}=-\frac{\partial\overline{P}}{\partial x}-\frac{\partial\overline{u_x^2}}{\partial x}-\frac{1}{r}\frac{\partial}{\partial r}\left(r\overline{u_xu_r}\right). \tag{2.2}$$

Using the above scales to order the terms of the x-momentum equation and retaining only the terms of highest order reduces (2.2) to

$$\overline{U}_x\frac{\partial\overline{U}_x}{\partial x}+\overline{U}_r\frac{\partial\overline{U}_x}{\partial r}=-\frac{1}{r}\frac{\partial}{\partial r}\left(r\overline{u_xu_r}\right). \tag{2.3}$$

The mean radial (r) momentum equation is

$$\overline{U}_x\frac{\partial\overline{U}_r}{\partial x}+\overline{U}_r\frac{\partial\overline{U}_r}{\partial r}=-\frac{\partial\overline{P}}{\partial r}-\frac{\partial\overline{u_xu_r}}{\partial x}-\frac{1}{r}\frac{\partial(r\overline{u_r^2})}{\partial r}+\frac{\overline{u_\theta^2}}{r}. \tag{2.4}$$

If, again, the terms are ordered as above, and only those of leading order retained, the result is

$$\begin{aligned}\frac{\partial\overline{P}}{\partial r}&=-\frac{1}{r}\frac{\partial}{\partial r}\left(r\overline{u_r^2}\right)+\frac{\overline{u_\theta^2}}{r}\\&=-\frac{\partial\overline{u_r^2}}{\partial r}+\frac{\overline{u_\theta^2}-\overline{u_r^2}}{r}.\end{aligned} \tag{2.5}$$

The $\overline{u_\theta^2}$ and $\overline{u_r^2}$ Reynolds stresses are nearly equal across the entire jet (Wygnanski & Feidler 1969) and so (2.5) can be further reduced to get

$$\frac{\partial\overline{P}}{\partial r}=-\frac{\partial\overline{u_r^2}}{\partial r}, \tag{2.6}$$

which relates the change in pressure to the transverse gradients in the $\overline{u_r^2}$ Reynolds stress. The terms in this equation are comparable in order to the leading-order terms in the x-momentum equation, (2.3) above. One can integrate (2.6) to yield

$$\begin{aligned}\overline{P}+\overline{u_r^2}&=\text{const.}\\&=0\end{aligned} \tag{2.7}$$

which clearly shows that as one approaches the jet axis from far away (where $\overline{P} = 0$), the mean pressure drops in proportion to the increase in $\overline{u_r^2}$. As a result, the minimum mean pressure will typically occur in the core of the jet where the turbulence level is greatest.

When the jet interacts with the free surface, the free-surface boundary conditions are imposed on the flow. It will be assumed that the Froude number is low, so that the free surface will remain flat. Under these circumstances, the kinematic condition reduces to $\overline{W} = 0$ and the dynamic (zero-stress) condition reduces to $\partial\overline{U}/\partial z = \partial\overline{V}/\partial z = 0$, both applied at the free surface. The Reynolds stresses of interest are required to satisfy the conditions $\overline{w^2} = \overline{vw} = 0$ and $\partial\overline{v^2}/\partial z = 0$. When these conditions are applied to the flow, a layer of thickness $\delta \ll x$ will develop near the free surface. This layer will grow laterally at a higher rate than the subsurface portion of the jet, and will have a lateral length scale ℓ_s which is larger than ℓ, the scale of the subsurface portion of the jet. A schematic of the resulting flow is shown in figure 1(*b*).

The following analysis will examine the region far enough downstream of the jet exit that h/x is small (where h is the depth of the jet axis beneath the free surface – see figure 2*b*), and the maximum axial velocity $U_\circ$ occurs near the free surface. Here, the velocity scales $U_\circ$ and $u_\circ$, used in the deep-jet analysis, are also appropriate for the near-surface region. This behaviour occurs for $x/h > 10$, roughly (see Walker *et al.* 1995). In this streamwise region, outside the near-surface layer, the jet will behave as a deep jet; that this is true will be shown below. Using the length scales δ and ℓ_s to non-dimensionalize the terms in the continuity equation indicates that the scale for the horizontal mean velocity $\overline{V}$ is $U_\circ \ell_s/x$, and the scale for the vertical mean velocity $\overline{W}$ is $U_\circ \delta/x$. Hence, in this region $\overline{W} \ll \overline{U}$. At this point the magnitude of ℓ_s is undetermined; however, it is expected to be smaller than x.

The above scaling can be applied to the momentum equations to identify the dominant terms in the near-surface region. The x-direction momentum equation is given by

$$\begin{array}{ccccccccc} \overline{U}\dfrac{\partial\overline{U}}{\partial x} + \overline{V}\dfrac{\partial\overline{U}}{\partial y} & + & \overline{W}\dfrac{\partial\overline{U}}{\partial z} & = & -\dfrac{\partial\overline{P}}{\partial x} & - \dfrac{\partial\overline{u^2}}{\partial x} & - \dfrac{\partial\overline{uv}}{\partial y} & - \dfrac{\partial\overline{uw}}{\partial z}. \\ O(1) \quad O(1) & & O\left(\dfrac{\partial\overline{U}/\partial z}{U_\circ/\delta}\right) & & O\left(\dfrac{\overline{P}}{U_\circ^2}\right) & O\left(\dfrac{u_\circ^2}{U_\circ^2}\right) & O\left(R_{uv}\dfrac{u_\circ^2}{U_\circ^2}\dfrac{x}{\ell_s}\right) & O\left(R_{uw}\dfrac{u_\circ^2}{U_\circ^2}\dfrac{x}{\delta}\right) \end{array} \tag{2.8}$$

The leading-order terms in this equation are $O(U_\circ^2/x)$; normalizing by this quantity yields the order-of-magnitude estimates which appear in the second line of (2.8). Here R_{uv} and R_{uw} are correlation coefficients for the indicated velocity fluctuations. The first two terms on the left of (2.8) are $O(1)$. If the free surface was a no-slip boundary, the third term on the left would be $O(1)$; however, since the free-surface boundary condition requires $\partial\overline{U}/\partial z = 0$ (at the surface), we can expect that $\partial\overline{U}/\partial z \ll U_\circ/\delta$ and so the third term in (2.8) will be negligible. It will be shown in the next paragraph that the pressure $\overline{P}$ will be on the order of $u_\circ^2$, and so the pressure gradient term will be $O(u_\circ^2/U_\circ^2)$. R_{uv} is by definition less than unity, but will, nonetheless, be $O(1)$, and therefore the second-to-last term will be $O(1)$. Since $\partial\overline{U}/\partial z$ is small it is expected that $R_{uw} \sim O(10^{-1})$, at most. Retaining only terms of leading order yields

$$\overline{U}\frac{\partial\overline{U}}{\partial x} + \overline{V}\frac{\partial\overline{U}}{\partial y} = -\frac{\partial\overline{uv}}{\partial y} - \frac{\partial\overline{uw}}{\partial z}, \tag{2.9}$$

which is the appropriate form for the x-momentum equation in the thin near-surface layer.

The z-momentum equation, in Reynolds-averaged form, is given by

$$\begin{array}{cccccccc} \overline{U}\dfrac{\partial \overline{W}}{\partial x} + \overline{V}\dfrac{\partial \overline{W}}{\partial y} + \overline{W}\dfrac{\partial \overline{W}}{\partial z} = -\dfrac{\partial \overline{P}}{\partial z} & & -\dfrac{\partial \overline{uw}}{\partial x} & & -\dfrac{\partial \overline{vw}}{\partial y} & & -\dfrac{\partial \overline{w^2}}{\partial z}, \\ O\left(\dfrac{\delta}{x}\right) & O\left(\dfrac{\delta}{x}\right) & O\left(\dfrac{\delta}{x}\right) & O\left(\dfrac{\overline{P}}{U_\circ^2}\dfrac{x}{\delta}\right) & O\left(R_{uw}\dfrac{u_\circ^2}{U_\circ^2}\right) & O\left(R_{vw}\dfrac{u_\circ^2}{U_\circ^2}\dfrac{x}{\ell_s}\right) & O\left(\dfrac{u_\circ^2}{U_\circ^2}\dfrac{x}{\delta}\right) \end{array} \tag{2.10}$$

with the order-of-magnitude estimates again on the second line, again normalized by U_o^2/x. The leading-order term in (2.10) is clearly the last one, the vertical $\overline{w^2}$ Reynolds-stress gradient. Since there are no significant lateral gradients in $\overline{W}$ or vertical gradients in $\overline{V}$, v and w are uncorrelated and $R_{vw} \ll 1$ (see e.g. Anthony & Willmarth 1992). Hence, all the other terms are of lower order than the $\overline{w^2}$ gradient, with the exception of $\partial \overline{P}/\partial z$, which is of undetermined order. The conclusion is that the vertical Reynolds-stress gradient, then, must be balanced by the vertical mean-pressure gradient. This requires that $\overline{P} \sim u_\circ^2$, as stated above, and indicates that the z-momentum equation, to leading order, reduces to

$$\frac{\partial \overline{P}}{\partial z} = -\frac{\partial \overline{w^2}}{\partial z}. \tag{2.11}$$

At a given streamwise position, this can be integrated to yield

$$\overline{P}(y,z) = \overline{P}_\infty(y) + \overline{w^2}_\infty(y) - \overline{w^2}(y,z) \tag{2.12}$$

for the pressure in the near-surface layer. Here the ∞ subscript represents a quantity evaluated for $z \to -\infty$, relative to the thin near-surface layer; i.e. deeper than the near-surface layer. The major conclusion to be obtained from the z-momentum equation is that the mean pressure $\overline{P}$ in the near-surface region is completely determined by the local $\overline{w^2}$ and the conditions at $z \to -\infty$, which, in this case, is the portion of the jet which still behaves as a deep jet.

It is anticipated that there will be a larger-magnitude outward $\overline{V}$ in the near-surface layer (and as a result of continuity, a larger lateral length scale ℓ_s) than exists in the deep jet. The exact relationship of these near-surface scales to those in the deep jet remains to be determined. The y-momentum equation is given by

$$\begin{array}{cccccccc} \overline{U}\dfrac{\partial \overline{V}}{\partial x} + \overline{V}\dfrac{\partial \overline{V}}{\partial y} + \overline{W}\dfrac{\partial \overline{V}}{\partial z} = -\dfrac{\partial \overline{P}}{\partial y} & & -\dfrac{\partial \overline{uv}}{\partial x} & & -\dfrac{\partial \overline{v^2}}{\partial y} & & -\dfrac{\partial \overline{vw}}{\partial z} \\ O\left(\dfrac{\ell_s}{x}\right) & O\left(\dfrac{\ell_s}{x}\right) & O\left(\dfrac{\partial \overline{V}/\partial z}{U_\circ/\delta}\right) & O\left(\dfrac{u_\circ^2}{U_\circ^2}\dfrac{x}{\ell_s}\right) & O\left(R_{uv}\dfrac{u_\circ^2}{U_\circ^2}\right) & O\left(\dfrac{u_\circ^2}{U_\circ^2}\dfrac{x}{\ell_s}\right) & O\left(R_{vw}\dfrac{u_\circ^2}{U_\circ^2}\dfrac{x}{\delta}\right), \end{array} \tag{2.13}$$

where the second line again contains the order-of-magnitude estimates normalized by $U_\circ^2/x$. The last term on the left-hand side of (2.13) can be neglected via the same reasoning which was applied to the corresponding term in the x-momentum equation, (2.8). The term containing the $\overline{vw}$ Reynolds stress will also be negligible since v and w are uncorrelated. Since $R_{uv} < 1$ and $x/\ell_s > 1$, the $\overline{uv}$ term is of lower order than the lateral pressure and $\overline{v^2}$ gradients, and can be neglected.

If, in addition to the foregoing, ℓ_s/x is assumed small, as it was for the deep jet, (2.13) reduces to

$$\frac{\partial \overline{P}}{\partial y} = -\frac{\partial \overline{v^2}}{\partial y}, \tag{2.14}$$

which is the result for the deep jet (compare to equation (2.6)). Combining (2.13) with (2.12) (along with equation (2.17) below for $\overline{P}_\infty$) and assuming that $\overline{v^2_\infty} \approx \overline{w^2_\infty}$ which is true for the deep jet, yields the result $\overline{v^2} \approx \overline{w^2}$ for the near-surface layer. This result is inconsistent with both the free-surface boundary conditions, and the observed behaviour of the Reynolds stresses near the surface, in low-Froude-number flows. This inconsistency indicates that ℓ_s cannot be so small that the advection terms on the left-hand side of the y-momentum equation can be neglected.

If ℓ_s is not negligibly small, then for the remaining terms in (2.13) to balance requires that $\ell_s/x \sim u_\circ/U_\circ$. The resulting form of the y-momentum equation is

$$\overline{U}\frac{\partial \overline{V}}{\partial x} + \overline{V}\frac{\partial \overline{V}}{\partial y} = -\frac{\partial \overline{P}}{\partial y} - \frac{\partial \overline{v^2}}{\partial y}. \tag{2.15}$$

In this equation, the imbalance between the lateral gradient of the pressure prescribed by (2.12) and the lateral $\overline{v^2}$ gradient will result in an outward acceleration in the plane of the free surface. It is this acceleration which results in the surface current.

It is useful to proceed one step further, combining the z- and y-momentum equations. Using (2.12) to eliminate the local pressure from (2.15) yields

$$\overline{U}\frac{\partial \overline{V}}{\partial x} + \overline{V}\frac{\partial \overline{V}}{\partial y} = -\frac{\partial}{\partial y}\left(\overline{P}_\infty + \overline{w^2_\infty} - \overline{w^2}\right) - \frac{\partial \overline{v^2}}{\partial y}. \tag{2.16}$$

Outside this near-surface layer, the flow behaves as a deep jet, hence (2.7) yields

$$\overline{P}_\infty = -\overline{u^2_r}_\infty = -\frac{\overline{w^2}_\infty + \overline{v^2}_\infty}{2}. \tag{2.17}$$

(This results because the sum of the normal stresses is coordinate independent and, in addition, $\overline{u^2_\theta}_\infty \approx \overline{u^2_r}_\infty$; i.e. $\overline{w^2}_\infty + \overline{v^2}_\infty = \overline{u^2_r}_\infty + \overline{u^2_\theta}_\infty \approx 2\overline{u^2_r}_\infty$.) Upon substitution into (2.16), (2.17) yields

$$\overline{U}\frac{\partial \overline{V}}{\partial x} + \overline{V}\frac{\partial \overline{V}}{\partial y} = \frac{\partial}{\partial y}\left(\overline{w^2} - \overline{v^2} - \frac{\overline{w^2}_\infty - \overline{v^2}_\infty}{2}\right). \tag{2.18}$$

For $\overline{w^2}_\infty \approx \overline{v^2}_\infty$, this reduces to

$$\overline{U}\frac{\partial \overline{V}}{\partial x} + \overline{V}\frac{\partial \overline{V}}{\partial y} = \frac{\partial}{\partial y}\left(\overline{w^2} - \overline{v^2}\right), \tag{2.19}$$

which indicates that the anisotropy that develops in the near-surface region, and which causes $\overline{w^2}$ and $\overline{v^2}$ to differ substantially, results in the outward flow at the surface. The discussion of (2.14) further indicates that the outward flow will only be absent if the near-surface anisotropy is also absent. This is because, in this thin layer, only the vertical gradients in the Reynolds stresses are balanced by pressure changes, and so the lateral gradients in the Reynolds stresses can only be balanced by an outward acceleration of the flow.

The reasoning that led to (2.15) can be used to develop an estimate for the order of magnitude of the outward flow velocity, V_s. Continuity requires that $V_s \sim U_o\ell_s/x$, as stated above. If $\ell_s/x \sim u_\circ/U_\circ$, required if both sides of (2.15) are of comparable order, then $V_s/U_\circ \sim u_\circ/U_\circ$. Since $u^2_\circ/U^2_\circ \sim 10^{-1}$ it appears that $V_s/U_\circ \sim 10^{-1/2}$, which is roughly three times larger than the spreading velocity in the deep jet, where $V/U_\circ \sim 10^{-1}$. There is a corresponding three-fold increase in ℓ_s relative to ℓ. It can therefore be concluded that the presence of the free surface will result in a roughly

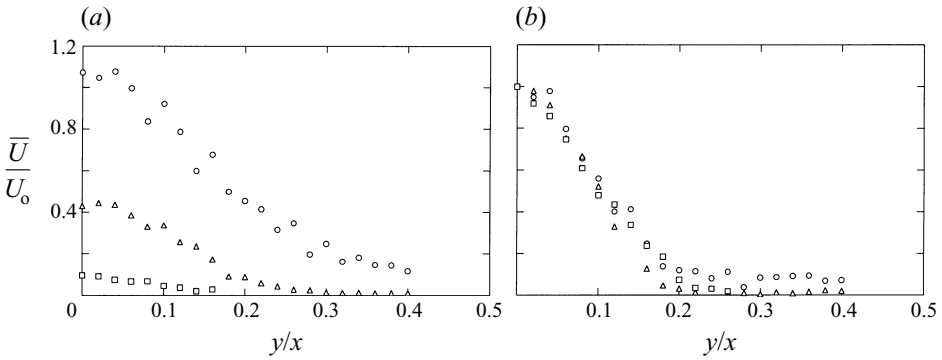

FIGURE 2. Profiles of mean streamwise velocity $\overline{U}/U_\circ$ versus transverse coordinate y/x at (*a*) the free surface ($z = 2d$), and (*b*) the centreplane ($z = 0$); □, $x/d = 8$; △, $x/d = 16$; ○, $x/d = 32$.

three-fold increase for both the outward velocity and the growth rate, as compared to a deep jet. These increases will be confined to a thin layer near the surface.

3. Comparison to experiment

Using data for the jet flows of Walker *et al.* (1995), the behaviour of a free-surface jet can be examined to see if the foregoing analysis is consistent with observed behaviour. The data for one of the cases examined in Walker *et al.* (1995) will be used – that for a jet issuing beneath and parallel to a free surface with a Froude number (Fr) of 1.0 and a Reynolds number (Re) of 12 700, both based on jet-exit velocity and exit diameter d. The depth of the jet axis below the free surface h is twice the jet-exit diameter. In dimensional terms, the jet had an exit diameter of 0.0254 m and an exit velocity of 0.50 m s^{-1}. The low Froude number for this jet is consonant with the assumptions in the foregoing analysis. Turbulence statistics were measured using a three-component laser velocimeter system; the experimental set-up and instrumentation are described in detail in Walker *et al.* (1995).

Figure 2 shows the mean streamwise velocity ($\overline{U}$) versus transverse position (y) for three streamwise locations in the plane of the free surface, $z = 2d$ (figure 2*a*), and in a horizontal plane passing through the jet axis, $z = 0$ (figure 2*b*). The vertical symmetry plane of the jet corresponds to $y = 0$, on the left edge of the figures. The three streamwise locations are $x/d = 8$, 16, and 32, which are just before the interaction of the jet with the free surface, just after interaction, and far enough downstream that the surface current is well established, respectively. Here, the y-coordinate has been normalized with the streamwise distance x, and the velocities have been normalized by the local streamwise velocity on the jet axis ($y = z = 0$). From figure 2(*b*), it can be concluded that well below the free surface, the jet remains self-similar since the profiles all collapse. The mean streamwise velocity at the free surface increases in magnitude with increasing x, until at $x/d = 32$ the maximum velocity at the free surface is comparable to that below the surface. In this region (near $x/d = 32$), the above analysis will be most applicable. At the free surface, we see that the lateral scale of the jet increases with increasing x and, at $x/d = 32$, is nearly twice that of the subsurface portion of the jet. This is consistent with the result above, indicating an increased growth rate for the surface-current layer. The self-similar behaviour below the surface is also consistent with the assumption that the jet evolves as a deep jet except in the near-surface layer.

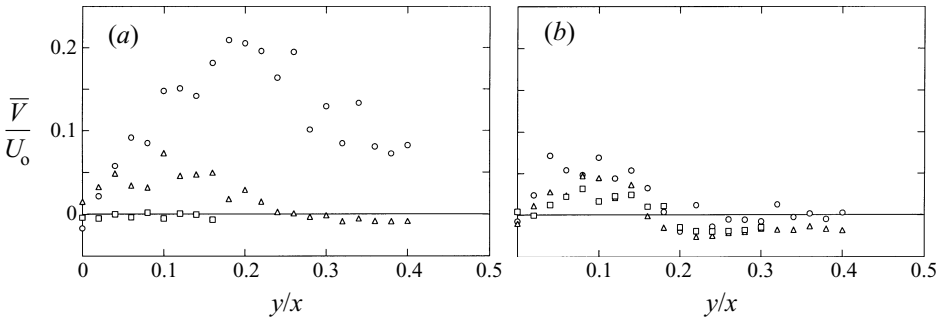

FIGURE 3. Profiles of mean transverse velocity $\overline{V}/U_\circ$ versus transverse coordinate y/x at (a) the free surface ($z = 2d$), and (b) the centreplane ($z = 0$); □, $x/d = 8$; △, $x/d = 16$; ○, $x/d = 32$.

The lateral mean velocity ($\overline{V}$) is shown in figure 3, with figure 3(a) showing results for $z = 2d$ and figure 3(b) those for $z = 0$. These data are normalized in the same way as those of figure 2. Although there is more scatter in these data than in the $\overline{U}$ velocities (due to the lower magnitude of these velocities), the subsurface flow clearly retains its self-similar character (figure 3b). At the free surface ($z = 2d$), the outward velocity is initially zero at $x/d = 8$, but increases at $x/d = 16$ and rises to 20% of the maximum axial velocity at $x/d = 32$. At this far downstream location, where one would expect the above analysis to be most applicable, the maximum outward velocity is roughly 3–4 times that in the deep jet, consistent with the above analysis, and with the observed increase in the horizontal length scale near the surface.

The above analysis indicates that, at the free surface, $\overline{V}^2$ will be of the same order as $(\overline{v^2} - \overline{w^2})$, provided that $\overline{w^2}_\infty = \overline{v^2}_\infty$. Figure 4 shows profiles of $(\overline{v^2} - \overline{w^2})$ for the locations examined above. For $y = 0$ (figure 4b), $(\overline{v^2} - \overline{w^2})$ is near zero, confirming that $\overline{v^2_\infty} \approx \overline{w^2_\infty}$, while at the free surface (figure 4a) it is initially small, but increases with streamwise distance. Also shown in figure 4(a), are lines indicating the maximum value of $\overline{V}^2$ using the data of figure 3(a). Initially, at $x/d = 8$, $\overline{V}^2_{max}$ is zero. As the level of $(\overline{v^2} - \overline{w^2})$ increases at $x/d = 16$, $\overline{V}^2_{max}$ increases slightly. At $x/d = 32$, where the above analysis should apply, the maximum in $(\overline{v^2} - \overline{w^2})$ is comparable to the maximum $\overline{V}^2$, as predicted.

These results indicate that the analysis of §2 is consistent with observation for the region near $x/d = 32$, where the mean and turbulent velocity scales for the near-surface flow are the same as those for the subsurface flow. The data show that the magnitude of the observed outward velocity relative to either the Reynolds-stress difference, or the spreading velocity of the deep jet, or the maximum streamwise velocity is as expected. The lateral scale of the near-surface flow also increases when compared to the subsurface flow, roughly as expected.

4. Discussion

The above analysis, and the resulting conclusions, can be related to earlier conjectures regarding the origin of the surface current. Primary among these are the observations of Anthony & Willmarth (1992), Walker *et al.* (1995) and Logory *et al.* (1996) that the surface current is related to the interaction of tangential vorticity with the free surface, and those of Launder & Rodi (1983) that the spreading near the surface in wall jets may be related to the production of streamwise (x-direction) vorticity owing to Reynolds-stress gradients. These will be addressed in turn.

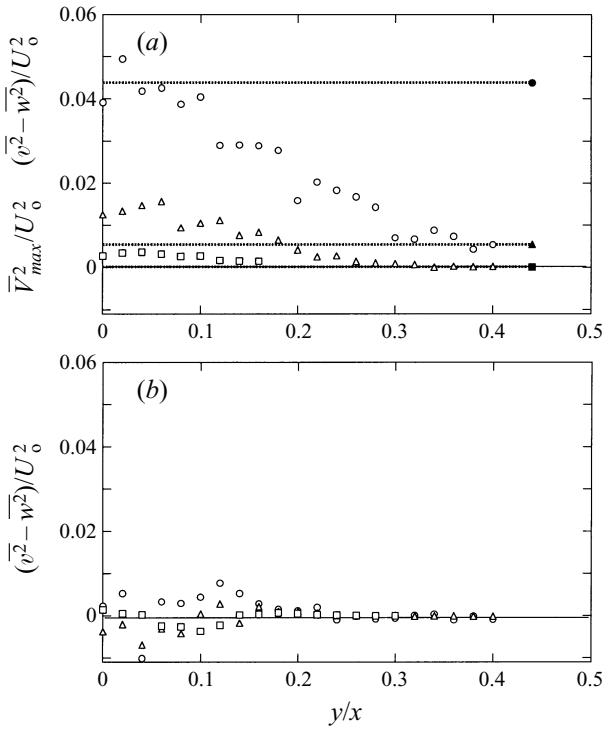

FIGURE 4. Profiles of Reynolds-stress difference $(\overline{v^2}-\overline{w^2})/U_\circ^2$ versus transverse coordinate y/x at (*a*) the free surface ($z = 2d$), and (*b*) the centreplane ($z = 0$); □, $x/d = 8$; △, $x/d = 16$; ○, $x/d = 32$. Lines and solid symbols in (*a*) indicate the maximum level of $\overline{V}^2/U_\circ^2$ at the free surface for the given x/d location.

The interaction of vorticity with a free surface can be identified with velocity–vorticity correlations which appear as source terms in the RANS equations. Walker *et al.* (1995) recast the Reynolds-stress terms from the Navier–Stokes equations in rotational form:

$$\frac{\partial \overline{u_i u_j}}{\partial x_j} = \frac{\partial k}{\partial x_i} - \epsilon_{ijk}\overline{u_j \omega_k}, \tag{4.1}$$

where $k = \overline{u_i u_i}/2$ and ω_i is the fluctuating vorticity. The velocity–vorticity correlations in (4.1) were discussed by Tennekes & Lumley (1972). They asserted that, in general, these correlations were small since the vorticity and velocity fluctuations occur on quite different spatial scales. Walker *et al.* (1995) argued that, near a free surface, the correlation of orthogonal components of the tangential velocity and vorticity would tend to be non-zero, owing to interaction of the local vorticity with its 'image' above the free surface. They showed that this was indeed true for the free-surface jet at low Froude number. Walker, Leighton & Garza-Rios (1996), in a study of initially homogeneous and isotropic turbulence near a free surface, showed that the correlation coefficient for orthogonal components of velocity and vorticity in planes parallel to the surface had a maximum of about 0.30–0.35 near the free surface, but was essentially zero elsewhere.

The relationship of these terms to the surface current, or more precisely, to the $(\overline{v^2}-\overline{w^2})$ Reynolds-stress difference which produces the surface current can be made

clear by first taking the curl of both sides of (4.1). This yields

$$\epsilon_{lmi}\frac{\partial}{\partial x_m}\left(\frac{\partial \overline{u_i u_j}}{\partial x_j}\right) = \epsilon_{lmi}\frac{\partial}{\partial x_m}\left(\frac{\partial k}{\partial x_i}\right) - \epsilon_{lmi}\frac{\partial}{\partial x_m}\left(\epsilon_{ijk}\overline{u_j\omega_k}\right)$$
$$= \frac{\partial}{\partial x_j}\left(\overline{u_j\omega_l} - \overline{u_l\omega_j}\right). \tag{4.2}$$

The streamwise component of this equation is

$$\frac{\partial^2 \overline{uw}}{\partial y\partial x} + \frac{\partial^2 \overline{vw}}{\partial y^2} + \frac{\partial^2 \overline{w^2}}{\partial y\partial z} - \frac{\partial^2 \overline{uv}}{\partial x\partial z} - \frac{\partial^2 \overline{v^2}}{\partial y\partial z} - \frac{\partial^2 \overline{vw}}{\partial z^2}$$
$$= \frac{\partial}{\partial y}\left(\overline{v\omega_x} - \overline{u\omega_y}\right) + \frac{\partial}{\partial z}\left(\overline{w\omega_x} - \overline{u\omega_z}\right), \tag{4.3}$$

which reduces to

$$\frac{\partial^2}{\partial y\partial z}\left(\overline{w^2} - \overline{v^2}\right) = \frac{\partial}{\partial y}\left(\overline{v\omega}_x - \overline{u\omega}_y\right) \tag{4.4}$$

at leading order. (It is assumed here that only orthogonal components of the surface-parallel velocity and vorticity are correlated, i.e. $\overline{u\omega_z} \approx 0$, $\overline{w\omega_x} \approx 0$.) Integrating (4.4) from far below the surface to a point in the near-surface layer yields

$$\frac{\partial}{\partial y}\left(\overline{w^2} - \overline{v^2}\right) = \frac{\partial}{\partial y}\left[\left(\widetilde{v\omega}_x - \widetilde{u\omega}_y\right)\delta\right] \tag{4.5}$$

for $\overline{v^2}_\infty \approx \overline{w^2}_\infty$. Here δ is the thickness of the near-surface layer and the velocity–vorticity correlations are now average values over the range of integration. Equation (4.5) indicates that the Reynolds-stress difference at the surface can equivalently be represented by the velocity–vorticity correlations (albeit, the average over the near-surface region in question, indicated here by the tilde). Since the vorticity and velocity fluctuations are correlated as a result of the proximity of the free surface, the origin of the surface current can equivalently be attributed to the interaction of the vorticity with the free surface or the stress anisotropy caused by the free surface.

Since both the vorticity/free-surface interaction and the anisotropy of the Reynolds stresses arise from the requirement that the surface-normal velocity vanish, the origin of the surface current can be traced ultimately to this boundary condition. This validates the conjecture of Anthony & Willmarth (1992) that this boundary condition was responsible.

Launder & Rodi (1984) conjectured that the outward flow in wall jets was due to the production of streamwise vorticity by Reynolds-stress gradients. (Actually the production term in question is the left-hand side of equation (4.3), above.) The production of streamwise vorticity, which requires both vertical and lateral gradients in the Reynolds stresses, then presumably leads to outward flow. The foregoing indicates that there is a more fundamental mechanism which causes the surface current – the direct production of outward momentum by lateral Reynolds-stress gradients.

5. Conclusions

In this study, the evolution of an initially axisymmetric jet interacting with a free surface was examined. The purpose was to determine the origin of the surface current – the large outward velocity which exists in a thin layer adjacent to the surface. In §2, the appropriate forms of the momentum equations for the near-surface region were

developed. These equations are valid for the region far-enough downstream of the jet exit that the maximum velocity occurs near the surface; $x/h > 10$, roughly. It was shown that near the surface, outward acceleration results from the balance between a positive contribution from the lateral gradients in the $\overline{v^2}$ Reynolds stress and a negative contribution from the lateral pressure gradient. The local pressure field near the free surface was shown to be largely determined by the level of $\overline{w^2}$. Combining these results indicated that the lateral acceleration was equal to the lateral gradient in the difference between $\overline{v^2}$ and $\overline{w^2}$, i.e. the stress anisotropy. Near the free surface, as a result of the boundary conditions, $\overline{w^2}$ becomes small, while $\overline{v^2}$ can actually increase, and the surface current results.

Comparison to available experimental data in §3 showed that the scaling assumptions used in the analysis were consistent with observed behaviour for $x/d = 32$. It also showed that, in this region, the square of the maximum outward velocity was comparable to the maximum in $(\overline{v^2} - \overline{w^2})$, and 3–4 times the outward velocity for a deep jet, as predicted by the theory. The lateral scale of the surface-current layer was seen to be about double that of the deep jet; the theory predicted that this would be roughly a factor of $10^{1/2}$.

It was also shown in §4 that the near-surface stress anisotropy could be related to the interaction of vorticity with the free surface via the velocity–vorticity correlations. This indicates that the idea of the surface current being caused by the stress anisotropy is consistent with earlier explanations in terms of vortex/free-surface interaction.

This is work was supported by the Office of Naval Research (ONR) under Contract No. N00014-96-C-0038 at ERIM, and Grant Nos. N00014-97-1-0053 and N00014-94-1-1083 at the University of Michigan, all monitored by Dr E. P. Rood. Some additional support was provided by the Program in Ocean Surface Processes and Remote Sensing under ONR University Research Initiative Grant No. N00014-92-J-1650, monitored by Drs D. Trizna and F. L. Herr.

REFERENCES

Anthony, D. G. & Willmarth, W. W. 1992 Turbulence measurements in a round jet near a free surface. *J. Fluid Mech.* **243**, 699–720.

Davis, M. R. & Winarto, H. 1980 Jet diffusion from a circular nozzle above a solid wall. *J. Fluid Mech.* **101**, 201–221.

Launder, B. E. & Rodi, W. 1983 The turbulent wall jet–measurements and modeling. *Ann. Rev. Fluid Mech.* **15**, 429–459.

Logory, L. M., Hirsa, A. & Anthony, D. G. 1996 Interaction of wake turbulence with a free surface. *Phys. Fluids* **8**, 805–815.

Mangiavacchi, N., Gundlapalli, R. & Akhavan, R. 1994 Dynamics of a turbulent jet interacting with a free surface. In *Free-Surface Turbulence* (ed. E. P. Rood & J. Katz). ASME-FED vol. 181, pp. 69–82.

Tennekes, H. & Lumley, J. L. 1972 *A First Course in Turbulence*. MIT Press.

Walker, D. T., Chen, C.-Y. & Willmarth, W. W. 1995 Turbulent structure in free-surface jet flows. *J. Fluid Mech.* **291**, 223–261.

Walker, D. T. & Johnston, V. G. 1991 Observations of turbulence near the free surface in the wake of a model ship. In *Dynamics of Bubbles and Vortices Near a Free Surface* (ed. I. Sahin & G. Tryggvason). ASME AMD-119.

Walker, D. T., Leighton, R. I. & Garza-Rios, L. O. 1996 Shear-free turbulence near a flat free surface. *J. Fluid Mech.* **320**, 19–51.

Wygnanski, I. & Fiedler, H. 1969 Some measurements in the self-preserving jet. *J. Fluid Mech.* **38**, 577–612.